

# Temperature and strain-rate effects on the fracture toughness of poly(ether ether ketone) and its short glass-fibre reinforced composite

J. Karger-Kocsis\* and K. Friedrich

Polymer and Composites Group, Technical University Hamburg-Harburg, 2100 Hamburg 90, FRG

(Received 27 November 1985; revised 17 February 1986)

Constant-strain-rate mechanical testing and surface fractography were used for the fracture mechanical characterization of poly(ether ether ketone) (PEEK) and its short glass-fibre reinforced composite. Testing was performed as a function of temperature, strain rate and heat treatment. The fracture toughness of both materials is highly dependent on these factors causing either brittle or ductile damage. At high strain rate, a brittle-ductile transition was observed in the  $K_{Ic}$ - $T$  curve of the PEEK matrix at 115°C. This could be interpreted as an isothermal-adiabatic transition superimposed on the glass transition. A similar, but less intense, transition was observed for the composite at higher temperature (roughly at  $T_g = 144^\circ\text{C}$ ). This shift in the real  $T_g$  region of PEEK can be explained by the presence of fibres which enhance the thermal conductivity, thus acting as heat sinks and drastically reducing the adiabatic heating effects of the crack tip. Heat annealing caused an increase in the crystallinity and a decrease in the fracture toughness. Reasonable agreement was found between the  $K_{Ic}$  values derived from the established  $J$  integral and those measured.

(Keywords: composite; fibre reinforcing; fracture toughness; poly(ether ether ketone); effects of temperature and strain rate)

## INTRODUCTION

Because of its excellent toughness, long-term thermal stability and solvent resistance, poly(ether ether ketone) (PEEK) has become a promising candidate for the production of new lightweight advanced composites. Results of investigations on structure and morphology<sup>1-6</sup> and on thermal behaviour<sup>7-11</sup> of PEEK have recently been published in the literature. Studies of the mechanical performance of PEEK focus on the effects of physical ageing<sup>10</sup>, fluid exposure<sup>12</sup> and hard radiation<sup>13,14</sup>, as one would expect for the matrix of a potential thermoplastic-based composite. Other information is available on the fracture and fatigue behaviour of discontinuous<sup>15,16</sup> and continuous<sup>17</sup> fibre-reinforced PEEK composites. Since PEEK is a high-temperature-resistant semicrystalline thermoplastic, the fracture characterization should, however, be extended to a broad temperature range, and also effects of heat ageing should be investigated in this respect. It is the objective of the present paper to contribute to the fracture mechanical characterization of PEEK and its short glass-fibre reinforced composites. In particular, temperature, strain-rate and annealing effects on the material's fracture toughness have been studied.

## EXPERIMENTAL

### General aspects

The fracture behaviour of neat PEEK (designated as matrix, M) and the 30 wt% short glass-fibre reinforced PEEK (composite, C) was studied by the use of compact tension (CT) specimens. Both PEEK materials are based

on Victrex 450 G PEEK of ICI Ltd, Wilton, UK. The CT specimens were cut from film-gated injection-moulded rectangular plaques. They were notched parallel to the mould flow direction (MFD) by means of a saw and designated as L cracked specimens (cf. Figure 1). Prior to the mechanical testing, the notch was sharpened with a razor blade.

The microstructure of the injection-moulded composite plaques was characterized in terms of the skin (S)-core (C) thickness, average fibre orientation ( $f_p$ ) in these regions, fibre length distribution, average fibre length<sup>16</sup> and degree of crystallinity. Results on the skin-core morphology across the plaque thickness ( $B$ ) as well as the  $f_p$  values were established by high-contrast scanning electron microscopy (SEM) of polished surfaces. Figure 1 shows the layered structure formed during injection moulding of the plaques and the geometry of the CT specimens used. The  $f_p$  value was calculated by the following equations<sup>18</sup>:

$$f_p = 2\langle \cos^2 \phi \rangle - 1 \quad (1)$$

$$\langle \cos^2 \phi \rangle = \frac{\sum_i N(\phi_i) \cos^2 \phi_i}{\sum_i N(\phi_i)} \quad (2)$$

where  $\phi_i$  is the angle between the individual fibres and the MFD, and  $N(\phi_i)$  is the number of fibres aligned at angle  $\phi_i$ .

The fibre length distribution was determined by means of light microscopy (LM) after burning off the matrix at about 700°C. A value for the degree of crystallinity could be derived from both density and differential scanning calorimetric (d.s.c.) measurements. Based on the work of

\*Humboldt fellow; on leave from Taurus Hungarian Rubber Works, Budapest, Hungary.

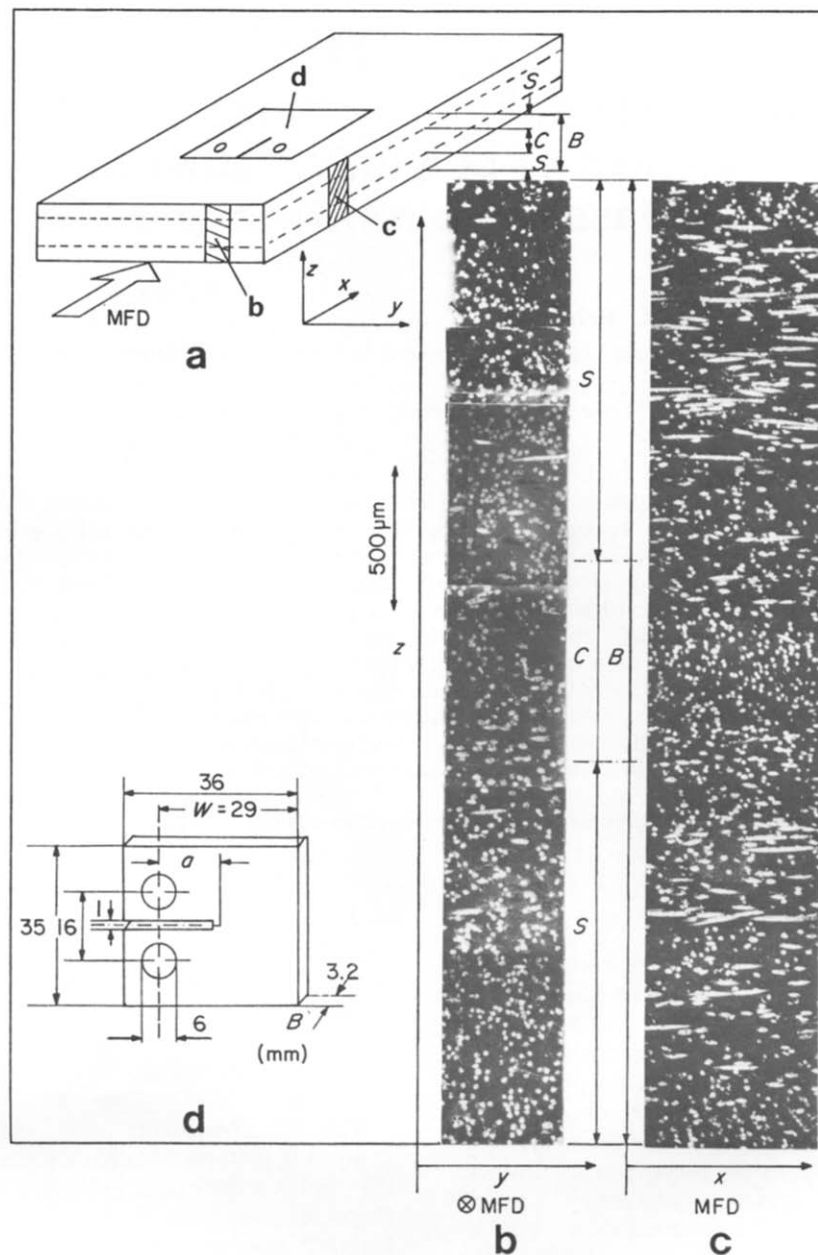


**Figure 1** (a) Direction of L cracks with respect to the plaque geometry. (b) Composite SEM micrograph of the layered structure in the z-y plane. (c) Composite SEM micrograph in the z-x plane. (d) Geometry of the CT specimen used

Blundell and Osborn<sup>2</sup> it was accepted that the densities of the fully amorphous and crystalline PEEK are 1.263 and 1.401 g cm<sup>-3</sup>, respectively, and the heat of fusion of the latter is 130 J g<sup>-1</sup>. The d.s.c. thermograms were recorded by a Hereus DTA 500 module connected to a TA 500 S device with a heating and cooling rate of 20 and 10°C min<sup>-1</sup>, respectively. Heat effects were calibrated by the heat of fusion of ultra-pure lead (m.p. 327.5°C; heat of fusion 22.6 J g<sup>-1</sup>).

**Fracture mechanical evaluation**

Loading of CT bars occurred in a Zwick 1445 type testing machine using crosshead speeds (*v*) of 1 and 10<sup>3</sup> mm min<sup>-1</sup>. At room temperature (RT), additional tests were carried out at *v*=10<sup>-1</sup>, 10 and 10<sup>2</sup> mm min<sup>-1</sup>. Variations of temperature in a broad range (-60 to +180°C) were achieved by the use of a thermostatically controlled chamber.

The fracture toughness (*K<sub>c</sub>*) was calculated by the following equation:

$$K_c = \frac{F_m}{BW} (a_i)^{1/2} f(a_i/W) \tag{3}$$

where *F<sub>m</sub>* is either the maximum load in a loading cycle or the intercept of the 95% slope with the load-displacement curve, according to the ASTM E 399 standard (the latter value was taken only for the neat PEEK fractured at *v*=10<sup>-1</sup> and 10 mm min<sup>-1</sup> at temperatures *T* ≥ RT and for both materials at *v*=10<sup>3</sup> mm min<sup>-1</sup> and *T* ≥ 120°C), *B* is the specimen thickness (3.2–3.5 mm), *W* is the specimen width (29 mm) (cf. Figure 1), *a<sub>i</sub>* is the actual crack length, and *f(a<sub>i</sub>/W)* is a polynomial geometrical correction (shape) factor<sup>19</sup>.

Fracture loading at 1 mm min<sup>-1</sup> crosshead speed was repeated on several CT bars of the PEEK composite in

order to establish the fluctuation of  $K_{Ic}$  values plotted against the  $a/W$  ratio. A few CT specimens precracked at  $v=1 \text{ mm min}^{-1}$  were finally fractured at  $10^3 \text{ mm min}^{-1}$  strain rate.

The  $J_{Ic}$  values of the materials at RT and  $v=1 \text{ mm min}^{-1}$  were determined from the  $R$  curve obtained by the multiple specimen technique according to the ASTM E 813 standard:

$$J = \frac{U}{B(W-a)} f(a/W) \quad (4)$$

where  $U$  is the area under the load-displacement curve, and the other parameters have already been defined in connection with equation (3).

For the calculation of the blunting line according to equation (5), literature values<sup>15</sup> for the yield stress ( $\sigma_y$ ) of the neat PEEK (100 MPa) and reinforced PEEK (150 MPa) were used:

$$J = 2\sigma_y \Delta a \quad (5)$$

The crack extension ( $\Delta a$ ) was established by LM after fracturing the specimens at  $10^3 \text{ mm min}^{-1}$  crosshead speed.

#### Failure analysis, fractography

Crack propagation paths were visualized on microphotographs taken by direct illumination by a Polyvar light microscope. The microscopic failure mode of the fractured specimens was studied on SEM microphotographs made by a Leitz REM 1600T scanning electron microscope. Prior to the SEM observations, the specimen surfaces were coated with gold in a sputtering chamber.

#### Heat treatment

For the solid-phase annealing, samples were kept at  $320^\circ\text{C}$  for 1.5 h, followed by an isothermal heat treatment at  $260^\circ\text{C}$  over 50 h (designated as 'a'). For comparison, other samples were quenched in water after heating up to  $320^\circ\text{C}$  for 20 min (designated as 'q').

## RESULTS AND DISCUSSION

#### Thermal behaviour

D.s.c. thermograms of the as-received (ar), quenched (q) and annealed (a) matrix as well as those of the composite were registered during heating and cooling (Figure 2). The d.s.c. traces of heating for both the annealed neat and reinforced PEEK show a more or less resolved double melting peak. This has been reported in the literature<sup>2,8</sup> and interpreted as a recrystallization phenomenon by Blundell and Osborn<sup>2</sup>. Based on transmission infra-red spectra of quenched PEEK, Nguyen and Ishida<sup>9</sup> supposed that this melting may be related to the rotation movement of the phenyl ether and benzophenone moieties of PEEK. However, the d.s.c. scans of samples annealed at different temperatures<sup>2</sup> show an intense splitting of the double peak, confirming the recrystallization process proposed by Holdsworth and Turner-Jones<sup>20</sup>. Our quenched samples show d.s.c. scans analogous to those of the 'as-received' ones (cf. Figure 2).

The volume fraction crystallinity ( $V_c$ ) was determined by density measurements assuming the two-phase model:

$$V_c = (\rho - \rho_a) / (\rho_c - \rho_a) \quad (6)$$

where  $\rho$ ,  $\rho_a$  and  $\rho_c$  are the densities of the actual, fully amorphous and fully crystalline phases, respectively. The value of  $V_c$  agrees well with the d.s.c. crystallinity based on the measured melt enthalpy ( $\Delta H_m$ ) of the samples (Table 1). There is also a good correlation between the d.s.c. crystallinity of the neat PEEK and that of the matrix of the glass-fibre reinforced composite (in the latter case the measured  $\Delta H_m$  was corrected with respect to the mass of the fibres). This is in contrast to the finding of Anderson *et al.*<sup>5</sup> who established by wide-angle X-ray studies that the crystallinity of the neat PEEK is greater than that of the matrix in the composite. Table 1 also reports the crystallization enthalpies ( $\Delta H_c$ ) of the samples. The d.s.c. traces registered in the cooling regime show that the crystallization of the neat PEEK begins earlier ( $300^\circ\text{C}$ ) than that of the matrix in the composite. In addition, the crystallization of the neat matrix takes place over a wider temperature range compared with the crystallization peak of the composite. There may be various reasons for these differences, for example effects of fibre coating on crystallization, possible nucleating agents in the neat matrix material and so on. At the moment, no final explanation can be given by the authors.

In spite of the enhanced crystallinity (cf. Table 1) of the annealed samples, no spherulites could be resolved by polarized LM. All the thermal characteristics, together with the other microstructural parameters of the samples used, are summarized in Table 1.

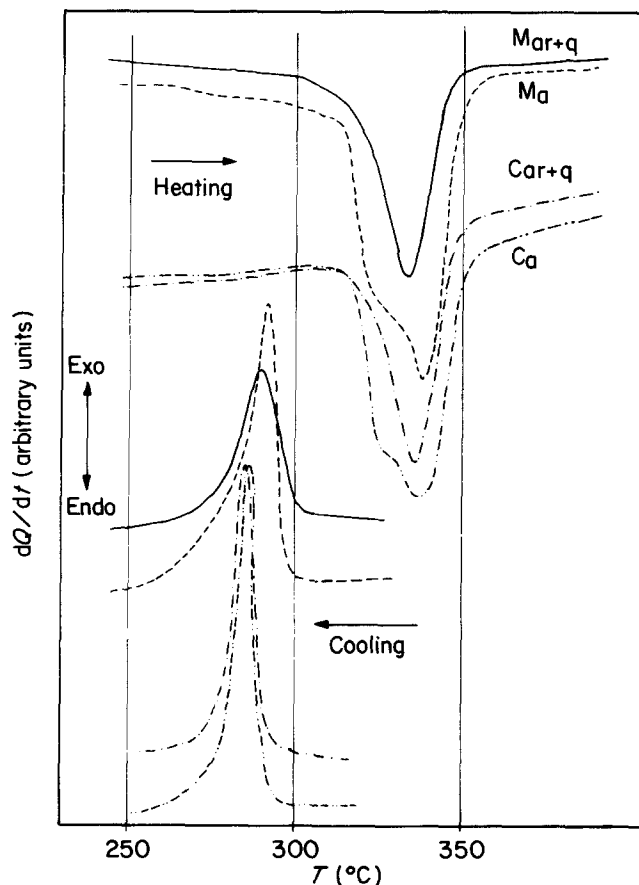


Figure 2 D.s.c. traces of the as-received (ar), quenched (q) and annealed (a) PEEK samples in heating and cooling regimes. Designation: M, matrix; C, composite

Table 1 Characterization of the PEEK samples used

Morphology, property	Matrix			Composite			
	ar	a	q	ar	a	q	
Layer structure, C/B		not investigated			0.17	0.17	0.17
Fibre orientation							
$f_{p,s}$	—	—	—	0.49	0.49	0.49	
$f_{p,c}$	—	—	—	-0.49	-0.49	-0.49	
Average fibre length ( $\mu\text{m}$ )	—	—	—	120	120	120	
Fibre aspect ratio	—	—	—	10-12	10-12	10-12	
Density ( $\text{g cm}^{-3}$ )	1.294	1.306	1.285	1.520	1.531	1.516	
Volume fraction crystallinity (%)	22.5	31.2	15.7	—	—	—	
$\Delta H_m$ ( $\text{J g}^{-1}$ )	31.4	39.1	32.0	20.7	27.6	18.6	
D.s.c. crystallinity <sup>a</sup> (%)	24.1	30.1	24.6	22.7	30.3	20.4	
$\Delta H_c$ ( $\text{J g}^{-1}$ )	30.7	38.5	32.5	20.1	22.9	20.0	
				(28.7) <sup>a</sup>	(32.7) <sup>a</sup>	(28.6) <sup>a</sup>	

<sup>a</sup> Related to the neat matrix (see text)

Effect of temperature on modulus, toughness and fracture energy

From the load-displacement curves registered during the measurements on the CT specimens, the initial slope ( $E_{in}$  in newtons per metre), the maximum load or the load at the intercept of the 95% slope of the curve ( $F_m$  in newtons) as well as the area under the curve up to  $F_m$  ( $A_m$  in joules) were read and calculated.  $E_{in}$  can be related directly to the 'elastic tensile modulus',  $F_m$  correlates with the 'fracture toughness' and  $A_m$  can be treated as the 'work of failure initiation'. Accepting the designation of Schultz and Friedrich<sup>21</sup>, these terms are referred to as  $E$ ,  $K_c$  and  $W$ , respectively. For demonstrating relative changes only, these values were normalized ( $E^x$ ,  $K_c^x$ ,  $W^x$ ) to a standard, for which the matrix values at RT and 1 mm min<sup>-1</sup> strain rate were chosen. Figure 3a shows the change in the normalized Young modulus ( $E^x$ ) with temperature ( $T$ ) at  $v = 1 \text{ mm min}^{-1}$ . Basically, analogous curves are available for  $K_c^x$  and  $W^x$  versus  $T$  (cf. Figures 3b and 3c). Each of these diagrams indicates that the properties of both the neat PEEK and its short-fibre reinforced version are dependent on the temperature in a way which could be expected from the thermal characteristics of PEEK. The monotonic decrease of  $E^x$  with  $T$  (Figure 3a) can be explained by the increasing thermoplasticity of the matrix. The observed fast drop in  $E^x$  above 120°C reflects the effect of the glass transition region ( $T_g = 144^\circ\text{C}$ ).

A formal comparison of the  $W^x$  term (Figure 3c) with a fracture energy value ( $G_c$ ) determined by simply using the relationship:

$$G_c = K_c^2/E \quad (\text{plane stress}) \quad (7)$$

in the standardized form ( $G_c^x = K_c^{x2}/E^x$ ) yields a good agreement between the as-calculated values ( $G_c^x$ , cf. Figure 4) and the measured ones ( $W^x$ , cf. Figure 3c).

Figure 5 shows the  $J-\Delta a$  curves for the materials investigated. For the points of the  $R$  curve of the composite a straight line could be easily fitted giving a  $J_{Ic}$  value of 3.5 kJ m<sup>-2</sup>. In the case of neat PEEK, on the other hand, only a few points in the  $\Delta a$  range between 0.5 and 1.2 mm could be taken into account; all the other ones were omitted owing to extensive tearing of the specimen (cf. values connected by the broken line in Figure 5) that altered the conditions from plane strain to plane stress. The regression line in this  $\Delta a$  range, which is

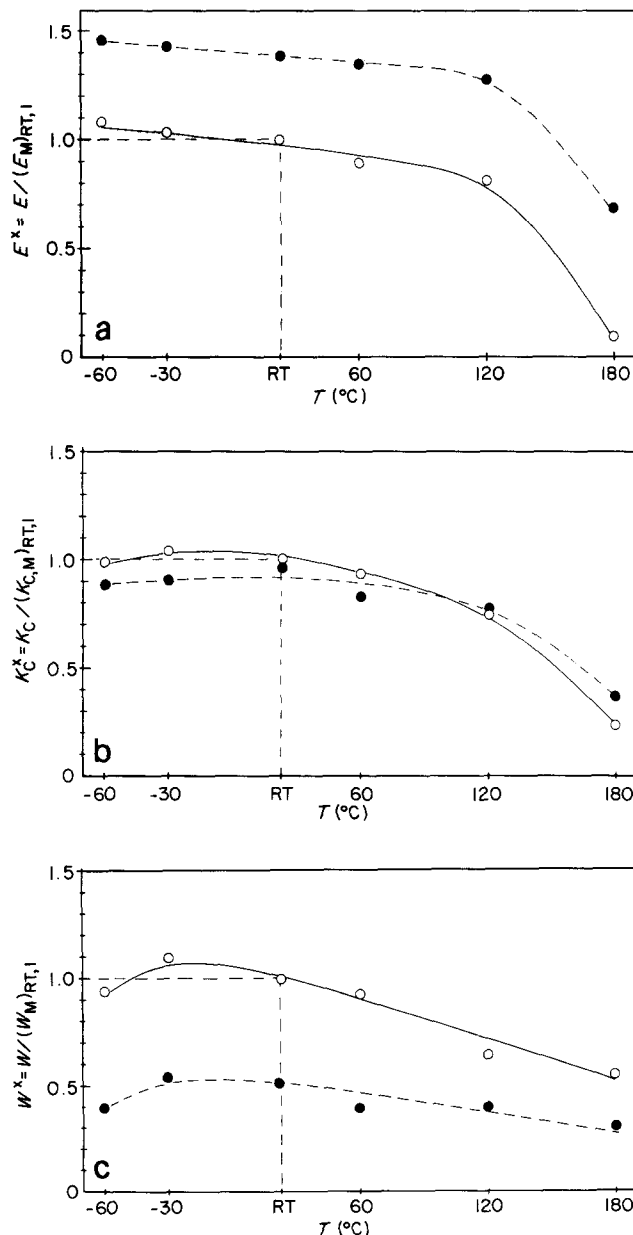


Figure 3 (a) Normalized tensile modulus ( $E^x$ ), (b) normalized fracture toughness ( $K_c^x$ ) and (c) normalized work of failure initiation ( $W^x$ ) vs.  $T$  curves of the neat PEEK and its composite at  $v = 1 \text{ mm min}^{-1}$  strain rate. The standardization values are:  $(E_M)_{RT,1} = 4.6 \times 10^5 \text{ N m}^{-1}$ ,  $(K_{c,M})_{RT,1} = 6.6 \text{ MPa m}^{1/2}$  and  $(W_M)_{RT,1} = 0.38 \text{ J}$ . Designation:  $\circ$ , matrix;  $\bullet$ , composite

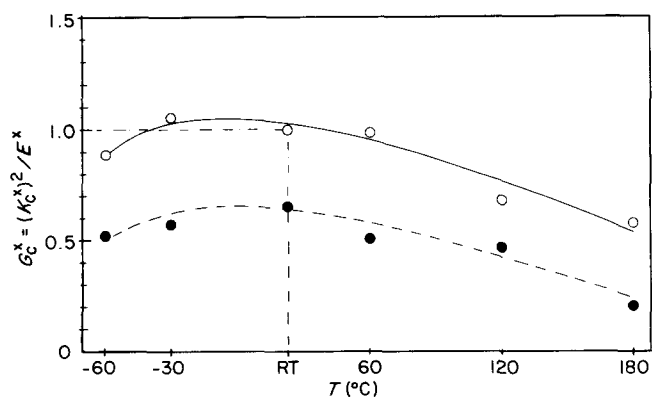


Figure 4 Normalized fracture energy ( $G_c^x$ ) vs.  $T$  curves of the neat PEEK and its composite at  $v=1 \text{ mm min}^{-1}$  strain rate. For designation, see Figure 3

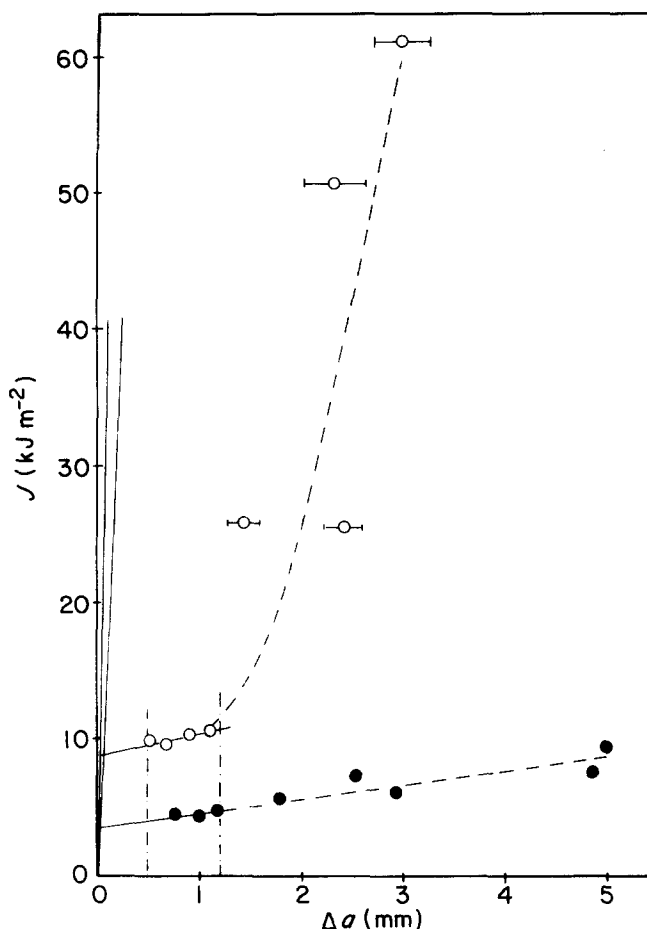


Figure 5  $J$ - $\Delta a$  curves for the PEEK samples at room temperature and  $v=1 \text{ mm min}^{-1}$  strain rate. For designation, see Figure 3

also recommended by the appropriate ASTM standard, gave  $8.7 \text{ kJ m}^{-2}$  for  $J_{Ic}$ . The normalized value of these evaluated  $J_{Ic}$  values,  $J_c^x = J_{Ic,C}/J_{Ic,M}$ , gives 0.4, which is in good agreement with both the  $G_c^x$  value (0.6, cf. Figure 4) and the  $W^x$  value (0.5, cf. Figure 3c).

It has to be mentioned that the size criteria for both  $B$  and  $W$  were fulfilled with our CT specimens for the  $J$  testing<sup>22</sup>, whereas for  $K_c$  evaluation only the  $W$  criterion was met. This means that our  $K_c$  values are greater than those strictly related to the plane strain condition<sup>15,22</sup>. In order to achieve reliable  $K_c$  values, the thickness of the CT specimens must be at least 10.9 and 4.3 mm for the neat PEEK and for the glass-fibre reinforced composite, respectively.

#### Influence of strain rate and temperature on the fracture toughness and failure mechanisms

Figure 6 illustrates the effect of temperature on the absolute values of  $K_c$  at two extremely different deformation rates ( $v=1$  and  $10^3 \text{ mm min}^{-1}$ ). The  $K_c$  values evaluated at lower  $v$  and at RT for the materials investigated agree very well with those calculated from the reported  $J_{Ic}$  values by using

$$K_c = (J_{Ic}E)^{1/2} \quad (\text{plane stress}) \quad (8)$$

Accepting that the  $E$  moduli of the neat and reinforced PEEK are 3.6 and  $10 \text{ GPa}$ <sup>23</sup>, equation (8) yields 5.6 and  $5.9 \text{ MPa m}^{1/2}$  for the neat PEEK and the 30% glass-fibre reinforced PEEK composite, respectively. These values are a little lower than the measured ones (6.6 and  $6.3 \text{ MPa m}^{1/2}$ ; cf. Figure 6) according to the size criteria predictions<sup>22</sup>.

Within the temperature range  $T < 60^\circ\text{C}$  it can be assumed that the calculated values are within the allowable limits of those fracture mechanics concepts which accept some degree of plasticity in the crack tip prior to crack instability<sup>24</sup>. In this temperature range, the effect of higher deformation rate results in a clear reduction of the material's fracture toughness. This could be expected from taking the time-dependent plasticity of polymeric materials into account.

With respect to the failure behaviour, it can be stated that the effects of temperature and strain rate are in principle the same as observed for other polymer systems<sup>25-27</sup>, i.e. a trend to brittle fracture with decreasing temperature and/or increasing strain rate, and a more ductile failure mode in the opposite direction. In particular, it was observed here that PEEK builds up a large plastic zone in front of the crack tip, even at temperatures far below RT, when the deformation rate is low. Also the fracture surfaces show evidence that PEEK retains its plasticity down to at least  $T = -60^\circ\text{C}$ . This is seen on the micrographs of Figure 7, which were taken from samples precracked at  $v=1 \text{ mm min}^{-1}$  and then totally fractured at  $v=10^3 \text{ mm min}^{-1}$ . In the region of low deformation rates (left sides of micrographs), a characteristic vein pattern (white zones) is found, indicating that an enormous amount of plastic flow of polymeric material has occurred prior to final separation. Although the density and thickness of the veins seems to increase with increasing  $T$ , no pronounced differences in

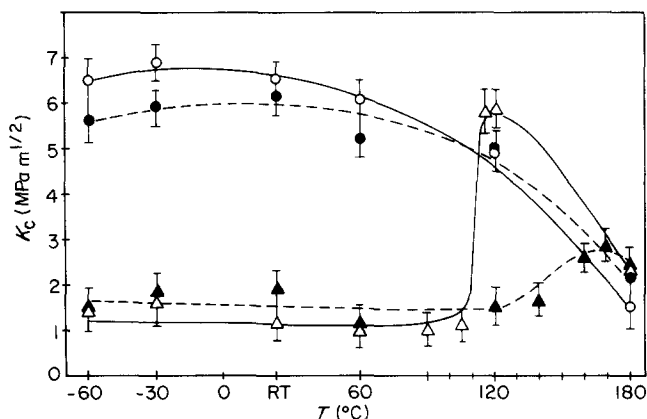


Figure 6  $K_c$  vs.  $T$  curves of the neat PEEK and its composite at  $v=1$  and  $10^3 \text{ mm min}^{-1}$  strain rate, respectively. Designation:  $\circ$ , matrix, and  $\bullet$ , composite, at  $v=1 \text{ mm min}^{-1}$ ;  $\triangle$ , matrix, and  $\blacktriangle$ , composite, at  $v=10^3 \text{ mm min}^{-1}$

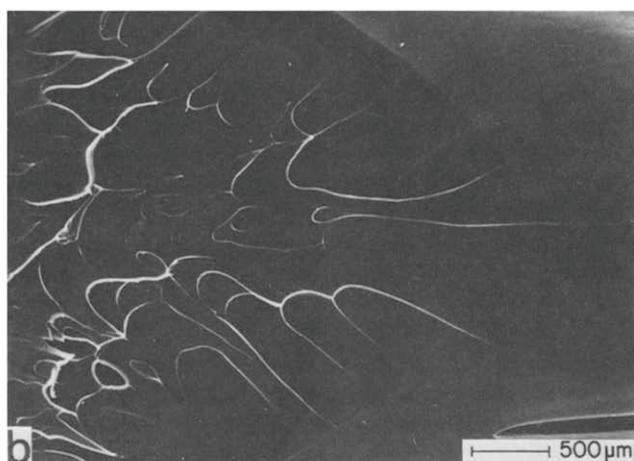
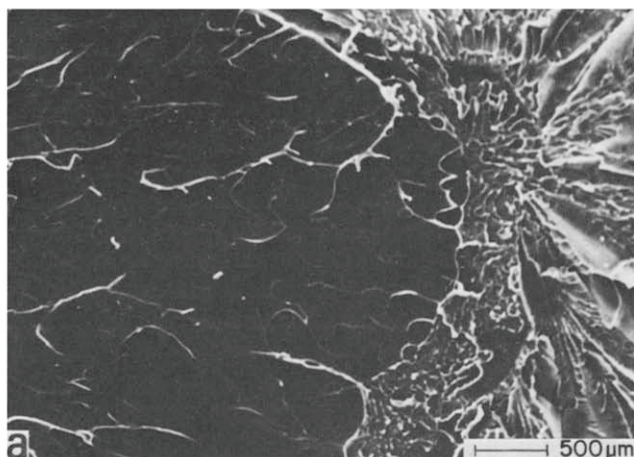


Figure 7 SEM micrographs of the fracture surface of the neat PEEK fractured at (a)  $-60^{\circ}\text{C}$  and (b)  $+60^{\circ}\text{C}$  in two steps with  $v=1$  and  $10^3 \text{ mm min}^{-1}$  strain rate

the  $K_{\text{c}}$  values were detected (at  $T = -60^{\circ}\text{C}$ ,  $K_{\text{c}} = 6.5 \text{ MPa m}^{1/2}$ ; at  $T = 60^{\circ}\text{C}$ ,  $K_{\text{c}} = 6.3 \text{ MPa m}^{1/2}$ ).

The right-hand sides of the micrographs in Figure 7 are related to the fracture of the precracked samples under high deformation rates ( $v = 10^3 \text{ mm min}^{-1}$ ). At  $T = -60^{\circ}\text{C}$  fracture occurs in a brittle manner, and the result is a rather low value of fracture toughness ( $K_{\text{c}} = 1.5 \text{ MPa m}^{1/2}$ ). At elevated temperature ( $T < 115^{\circ}\text{C}$ ) this type of fracture would also have dominated the breakdown process of PEEK if testing had been performed with a non-precracked sample. In the present situation, however, the predeformation at  $v = 1 \text{ mm min}^{-1}$ , associated with crack tip blunting and some undefined degree of orientation of the polymer, caused ductile failure with a corresponding  $K_{\text{c}}$  value of about  $8 \text{ MPa m}^{1/2}$ .

Returning to Figure 6, there is still the region  $T \geq 60^{\circ}\text{C}$  to discuss. Here, the low-velocity curves show a uniform, permanent reduction in  $K_{\text{c}}$ , as already discussed in connection with Figure 3b. The high-velocity curves, however, exhibit some kind of discontinuity, especially in the case of unreinforced PEEK. At  $T = 115^{\circ}\text{C}$  and velocity  $v = 10^3 \text{ mm min}^{-1}$ , the  $K_{\text{c}}$  values increase sharply from a level of around  $1.5 \text{ MPa m}^{1/2}$  (still at  $T = 105^{\circ}\text{C}$ ) to  $6.5 \text{ MPa m}^{1/2}$  within a temperature range of less than  $10^{\circ}\text{C}$ . This change in fracture toughness is associated with a plane strain–plane stress transition causing a change from brittle to ductile matrix failure, which usually occurs in the vicinity of the glass transition temperature of the

polymer ( $T_{\text{g PEEK}} = 144^{\circ}\text{C}$ ). It is assumed here that the shift in the ductile–brittle transition temperature down to  $T = 115^{\circ}\text{C}$  is a result of local, adiabatic heating at the notch tip due to the very rapidly introduced mechanical work. With a further increase in  $T$ , this toughness maximum drops again due to further softening of the matrix.

The  $K_{\text{c}}$  maximum for the composite lies at a higher temperature level (beginning at  $T \approx T_{\text{g PEEK}} = 144^{\circ}\text{C}$ )<sup>2</sup>. It is, however, much less pronounced compared with that of the PEEK matrix. This ductile–viscous rather than brittle–ductile transition can be explained by a decrease in the reinforcing effect due to the matrix, which becomes more and more viscous with increasing  $T$ . An isothermal–adiabatic transition is not expected for the composite, since the thermal conductivity of a glass-fibre filled system is usually higher than that of the neat polymer, so that in this system the fillers can act as heat sinks, dissipating the accumulated heat more effectively.

Another contributing factor is that the matrix volume fraction is reduced (the composite consists of 82 vol% matrix and 18 vol% glass-fibre reinforcement). Thus the heat accumulation for a potential isothermal–adiabatic transition as well as the possibility of matrix yielding is suppressed.

Figure 8 compares two low-magnification micrographs of composite fracture surfaces obtained after loading with  $v = 1 \text{ mm min}^{-1}$  at  $T = -60^{\circ}\text{C}$  and  $120^{\circ}\text{C}$ , respectively. It

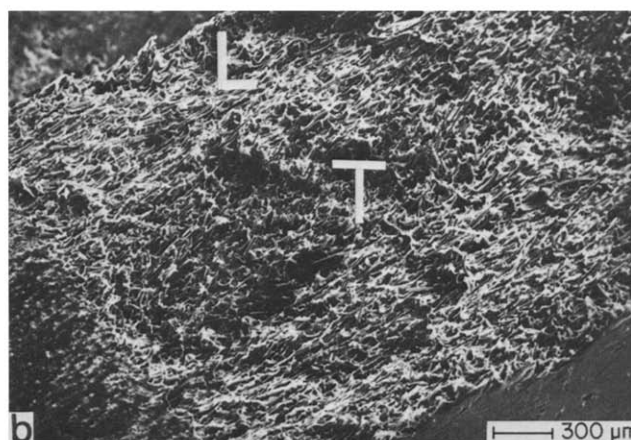
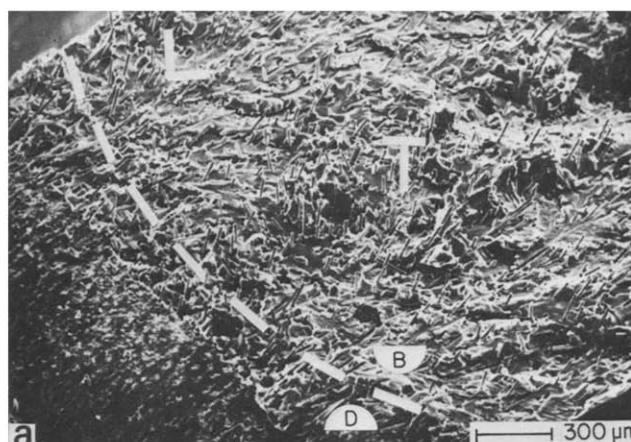


Figure 8 SEM micrographs of the fracture surface of the PEEK composite fractured with  $v = 1 \text{ mm min}^{-1}$  at (a)  $-60^{\circ}\text{C}$  and (b)  $+120^{\circ}\text{C}$ , respectively. Designation: L and T refer to the regions where the fibres are oriented longitudinally (parallel) and transverse (perpendicular) to the crack direction, respectively; D, ductile; B, brittle

can be seen that in the low-temperature case the matrix between many pulled-out fibres failed in a ductile mode at the beginning and finally in a brittle manner. The opposite, a totally ductile/viscous type of tearing of the polymer around and between the fibres, took place at elevated temperatures.

The effect of strain rate on the fracture mode is illustrated in Figure 9. Increasing the strain rate from  $v=1$  to  $10^3$  mm min<sup>-1</sup> causes a total embrittlement of the PEEK matrix between the fibres, which is more or less unaffected by testing temperatures below  $T=120^\circ\text{C}$ . This, in turn, is associated with a very low degree of fracture energy (relative to those samples broken at  $v=1$  mm min<sup>-1</sup>). In spite of the simultaneous increase in modulus with  $v$ , the enormous reduction in  $G_c$  finally also causes a very low value of  $K_{Ic}$ . Above  $120^\circ\text{C}$ , the fracture surface exhibits a stepwise change in character. It starts from a rather brittle/semiductile appearance and ends in a ductile/viscous matrix behaviour. This transition is associated with the observed  $K_{Ic}$  maximum within the temperature region around  $T \approx T_g$ .

Concerning the effect of  $v$  on  $K_{Ic}$  at  $T=RT$  in more detail (Figure 10), one finds that for both the neat and reinforced PEEK the reduction in toughness occurs monotonically with increasing  $v$ . In a single logarithmic plot, this appears, however, as a drop in  $K_{Ic}$  above  $v=10^2$  mm min<sup>-1</sup>. Below this velocity the  $K_{Ic}$  values of the neat matrix and of the composite vary around 7 MPa m<sup>1/2</sup>. The reduction in  $K_{Ic}$  can be explained by a

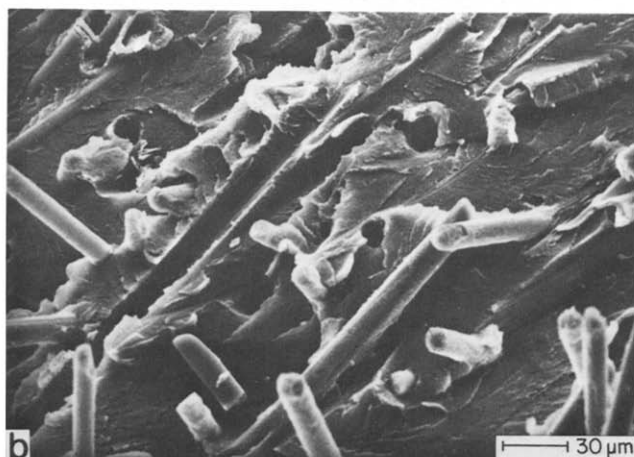
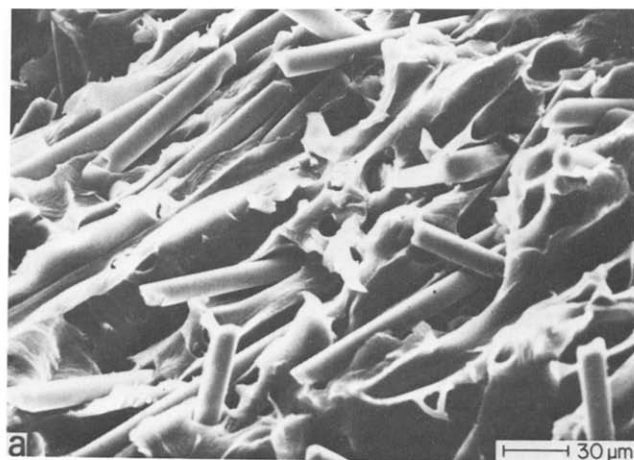


Figure 9 SEM micrographs of the L region of the fracture surface of the PEEK composite fractures with (a)  $v=1$  mm min<sup>-1</sup> and (b)  $v=10^3$  mm min<sup>-1</sup> strain rate at room temperature

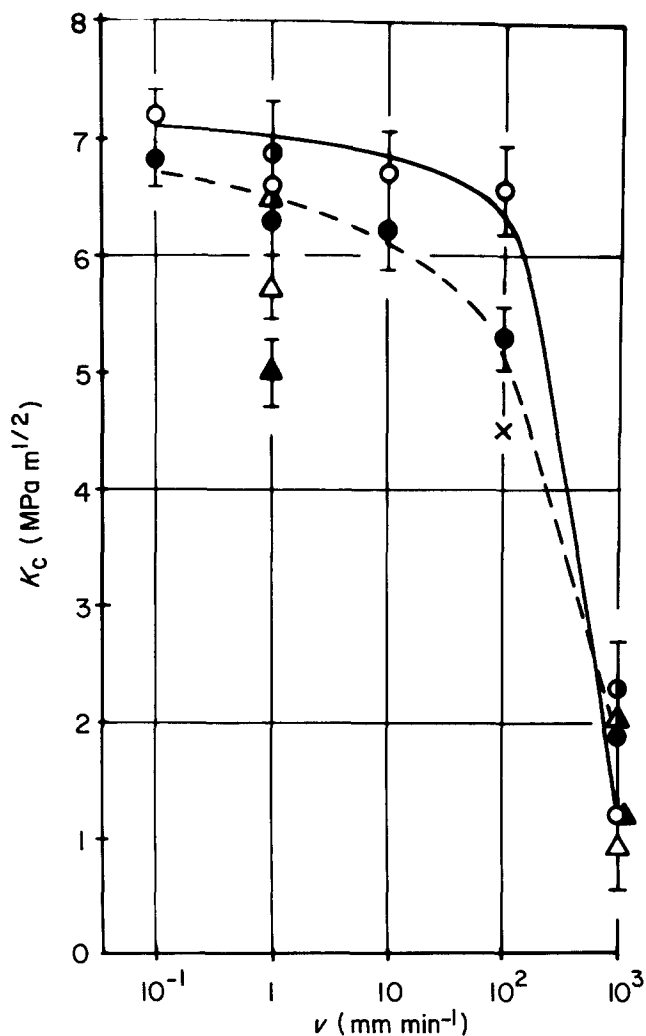


Figure 10 Variation of  $K_{Ic}$  vs. strain rate ( $v$ ) at room temperature for the neat and reinforced PEEK, as well as for their heat-treated versions. Designation: as-received— $\circ$ , matrix, and  $\bullet$ , composite; annealed— $\triangle$ , matrix, and  $\blacktriangle$ , composite; quenched— $\circ$ , matrix, and  $\blacktriangle$ , composite; literature value<sup>15</sup>— $\times$

reduced molecular mobility and thus a lower ductility of the matrix at higher loading velocities.

#### Variation of fracture behaviour due to different heat treatment

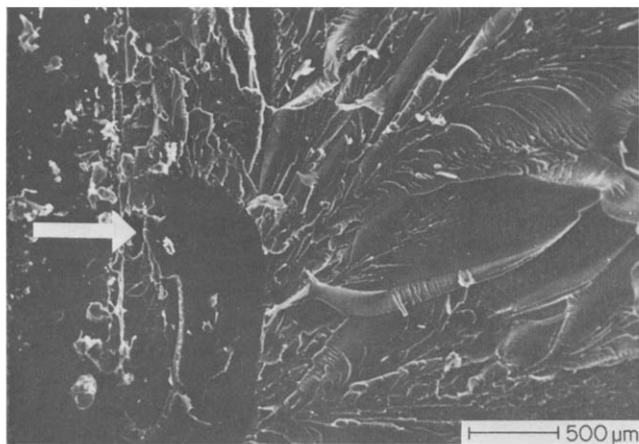
Figure 10 also shows the variation of  $K_{Ic}$  caused by the performed annealing and quenching processes. The  $K_{Ic}$  values for quenched and annealed specimens are summarized in Table 2. The results indicate that the fracture toughness increases with decreasing crystallinity of the matrix. Corresponding SEM photographs of the fracture surface of the heat-treated materials show evidence that the annealed samples have failed in a brittle manner (Figure 11). The quenched samples, on the other hand, show similar features to those observed for the as-received material under the same testing conditions (cf. Figure 7b). From these findings it should be concluded that for fracture toughness evaluation of semicrystalline polymers, especially for heat-resistant ones, the crystallinity of the matrix should always be taken into account.

#### CONCLUSIONS

The findings of this study on the fracture mechanical behaviour of PEEK and its short glass-fibre reinforced

**Table 2** The effect of annealing and quenching on the fracture toughness ( $K_{Ic}$ ) of the neat and reinforced PEEK at room temperature

	$K_{Ic}$ (MPa m <sup>1/2</sup> )			
	Matrix		Composite	
$v$ (mm min <sup>-1</sup> )	1	10 <sup>3</sup>	1	10 <sup>3</sup>
Annealed	5.7	0.9	5.0	1.2
As-received	6.6	1.2	6.3	1.9
Quenched	6.9	2.3	6.5	2.0

**Figure 11** SEM micrograph of the fracture surface of the annealed PEEK, fractured at room temperature with  $v = 1 \text{ mm min}^{-1}$  strain rate

composite can be summarized in the following form:

(i) *Low strain rate.* The fracture toughness ( $K_{Ic}$ ) of PEEK at rather low testing velocities ( $v = 1 \text{ mm min}^{-1}$ ) varies at  $T = \text{RT}$  around  $7 \text{ MPa m}^{1/2}$ . In this  $T$ - $v$  range,  $K_{Ic}$  is only slightly reduced by the addition of 30 wt% glass fibres. This reinforcement enhances the modulus of the material by about 50%. The  $K_{Ic}$  of both neat matrix and composite does not change very much when reducing the temperature down to  $-60^\circ\text{C}$  or increasing it up to  $60^\circ\text{C}$ . A further increase in  $T$  finally reduces the  $K_{Ic}$  values down to about  $2 \text{ MPa m}^{1/2}$  at  $180^\circ\text{C}$ , which is mainly due to a change in the deformation performance of the matrix from ductile to viscous. Additional determination of the  $J$  integral value of PEEK and its composite led to  $J_{Ic}$  values of  $8.7$  and  $3.5 \text{ kJ m}^{-2}$ , respectively. These values are in quite good agreement with corresponding values of  $K_{Ic}$  measurements.

(ii) *High strain rate.* An increase in strain rate to  $v = 10^3 \text{ mm min}^{-1}$  yields a clear reduction of the  $K_{Ic}$  values down to a level of  $1$ – $2 \text{ MPa m}^{1/2}$  for both materials. It is associated with an embrittlement of the polymer matrix which became evident up to  $T = 115^\circ\text{C}$  in the case of neat PEEK and  $T \approx T_g$  in the case of glass-fibre reinforced material. Above these threshold values a brittle-ductile and a brittle-ductile/viscous transition

was detected for the neat and reinforced PEEK, respectively, and interpreted.

(iii) *Heat annealing.* Some additional studies on the effect of thermal treatments on  $K_{Ic}$  showed that a small increase in crystallinity can cause a clear reduction of  $K_{Ic}$  associated with a ductile-brittle transition.

## ACKNOWLEDGEMENTS

J. Karger-Kocsis would like to thank the Alexander von Humboldt Foundation for the fellowship at the Polymer and Composites Group of the Technical University Hamburg-Harburg. Thanks are also due to ICI, Wilton, UK, for providing the test material. Part of the work was supported by the Deutsche Forschungsgemeinschaft (DFG FRI 675-1-1).

## REFERENCES

- Dawson, P. C. and Blundell, D. J. *Polymer* 1980, **21**, 577
- Blundell, D. J. and Osborn, B. N. *Polymer* 1983, **24**, 953
- Hay, J. N., Kemmish, D. J., Langford, J. I. and Rae, A. I. M. *Polymer* 1984, **25** (Commun.), 175
- Wakelyn, N. T. *Polymer* 1984, **25** (Commun.), 306
- Anderson, D. P., Kumar, S. and Adams, W. W. *Polym. Preprints* 1985, **26**, 275
- Rueda, D. R., Ania, F., Richardson, A., Ward, I. M. and Balta Calleja, F. J. *Polymer* 1983, **24** (Commun.), 258
- Attwood, T. E., Dawson, P. C., Freeman, J. L., Hoy, L. R. J., Rose, J. B. and Staniland, P. A. *Polymer* 1981, **22**, 1096
- Whitaker, R. B., Attalla, A., Sullenger, D. B., Wang, P. S., Dichiaro, J. V. and Kenyon, A. S., 16th National SAMPE Technical Conf., Albuquerque, New Mexico, 9–11 Oct. 1984
- Nguyen, H. X. and Ishida, H. *Polym. Preprints* 1985, **26**, 273
- Kemmish, D. J. and Hay, J. N. *Polymer* 1985, **26**, 905
- Velisaris, C. N. and Seferis, J. C., SPE ANTEC 1985, **31**, 401
- Stober, E. J., Seferis, J. C. and Keenan, J. D. *Polymer* 1984, **25**, 1845
- Yoda, O. *Polymer* 1985, **26** (Commun.), 16
- Sasuga, T. and Hagiwara, M. *Polymer* 1985, **26**, 501
- Jones, D. P., Leach, D. C. and More, D. R. *Polymer* 1985, **26**, 1385
- Friedrich, K., Walter, R., Voss, H. and Karger-Kocsis, J. *Composites* 1986, **17**, 205
- Leach, D. C. and Moore, D. R. *Composites Sci. Technol.* 1985, **23**, 131
- Rau, S., McGee, S. and McCullough, R. L. 'Determination of fibre orientation in short fibre composites', Center for Composite Materials Report No. CCM-80-11, University of Delaware, Newark, 1980
- Friedrich, K. *Composites Sci. Technol.* 1985, **22**, 43
- Holdsworth, P. J. and Turner-Jones, A. *Polymer* 1971, **12**, 195
- Schultz, J. M. and Friedrich, K. *J. Mater. Sci.* 1984, **19**, 2246
- Hashemi, S. and Williams, J. G. *J. Mater. Sci.* 1984, **19**, 3746
- 'Vitrex PEEK, A guide to grades for injection moulding', Prospect of ICI Ltd, VK2/1184, 1984
- Schwalbe, K.-H. 'Bruchmechanik metallischer Werkstoffe', Carl Hanser Verlag, München, 1980, p. 44
- Folkes, M. J. 'Short Fibre Reinforced Thermoplastics', Research Studies Press, Chichester, 1982
- Kinloch, A. J. and Young, R. J. 'Fracture Behaviour of Polymers', Applied Science Publ., London, 1983
- Kausch, H. H. 'Polymer Fracture', Springer, Berlin, 1978